

# Nonlinear Stability of Curved Multi-phase Composite Panels: Influence of Agglomeration in Randomly Distributed Carbon Nanotubes with Non-uniform In-plane Loads

## Abstract

The nonlinear stability characteristics of doubly curved panels made of three-phase composites with randomly dispersed carbon nanotubes (RD-CNTRFC) subjected to practically-relevant non-uniform in-plane loads are investigated in this study. Carbon nanotubes, when mixed with resin polymer, may give rise to bundles, termed as agglomerations, which can have a profound impact on the effective material properties. There exists a strong rationale to investigate the influence of such agglomeration on the nonlinear equilibrium path of panels, which can subsequently be included in the structural stability design process to enhance operational safety. A multi-stage bottom-up numerical framework is developed here to probe the nonlinear stability characteristics. The effective material properties of RD-CNTRFC panels are determined using the Eshelby-Mori-Tanaka approach and the Chamis method of homogenization. By considering von-Kármán non-linearity and Reddy's higher-order shear deformation theory, strain-displacement relations are established for the non-linear stability analysis. The governing partial differential equations are simplified into nonlinear algebraic relations using Galerkin's method. Subsequently, by reducing the stiffness matrix neglecting the non-linear terms and solving the Eigenvalue problem, we obtain critical load and non-linear stability path of shell panels based on arc-length approach. In the present study, various shell geometries such as cylindrical, elliptical, spherical and hyperbolic shapes are modeled along with the flat plate-like geometry to investigate the non-linear equilibrium paths, wherein a geometry-dependent programmable softening and hardening behavior emerges.

**Keywords:** Doubly curved shells, Randomly distributed carbon nanotubes, Post-buckling analysis of composites, Three-phase composites, Programmable softening and hardening behaviour

## 45    **1. Introduction**

46            Shell panels are a critical structural component in the design of aircraft wings, forming the  
47 flaps and membranes. These panels are typically thin-walled structures and are often supported with  
48 stiffeners or stringers to enhance structural stiffness. However, this additional support increases the  
49 overall weight of the structure significantly. Carbon nanotubes (CNTs) offer a promising solution by  
50 improving the stiffness of composite panels without the need for additional stringers, providing high  
51 flexural resistance under both static and dynamic loads. Past experiences have shown that these thin-  
52 walled structures can become vulnerable under in-plane compression loads (Reddy, 2003),  
53 potentially leading to catastrophic failures during operation. Moreover, the in-plane loading applied  
54 to these components can be non-uniform, depending on the stiffness of neighboring elements,  
55 complexity of the adjacent structural configuration and surrounding loading conditions. Therefore,  
56 addressing the stability criteria of thin-walled structures becomes crucial. In this context, the present  
57 study delves into the stability performance of randomly distributed carbon nanotube-reinforced  
58 composite shell panels when subjected to non-uniform in-plane loadings. Investigating the influence  
59 of CNT aggregation on stability performance is of great significance for aircraft designers, as it aids  
60 in accurately predicting the stability performance of CNT-based composite panels considering real-  
61 world manufacturing complications. The current study focuses on investigating the non-linear  
62 stability of carbon nanotube (CNT) reinforced shell panels like Cylindrical, Spherical, Elliptical, and  
63 Hyperbolic in geometry, considering the random distribution of nanotubes in the polymer matrix.

64            In general, thin-walled structures are susceptible to losing stability when subjected to a  
65 critical amount of in-plane compressive load (Garg et al. 2022; Dey et al. 2018b). This phenomenon  
66 is known as buckling and can result in the structure undergoing significant deformation during the  
67 post-buckling regime or even collapsing under further loads. As a result, researchers need to consider  
68 the post-buckling behavior when designing and analyzing thin-walled structures to ensure they can  
69 withstand the expected loading conditions and maintain stability. The members may lose one stable  
70 configuration and attain another stable configuration. The load at which it changes from one stable  
71 configuration to another is known as critical load or buckling load, while the member may withstand

72 a higher amount of load and undergo large deformation. Such reserve strength is gained through a  
73 post-buckling path or non-linear equilibrium path (Reddy, 2003). The current study probes the post-  
74 buckling strength of different types of shell panels, including Cylindrical, Spherical, Elliptical, and  
75 Hyperbolic, where randomly distributed carbon nanotubes are investigated as reinforcement. Apart  
76 from aerospace applications, these thin-walled structures are widely used as structural members in  
77 the broader field of engineering, such as Automobile, Marine, Civil, and Mechanical Engineering,  
78 due to their combination of strength and lightweight characteristics. Despite their advantages, it is  
79 important to consider the post-buckling behavior of thin-walled structures to ensure they maintain  
80 stability under the expected loading conditions. Thus, enhancement of the buckling behavior has  
81 been a center of focus of the research community. To this end, different reinforcements have been  
82 used including CNTs and different forms of graphene derivatives (Chandra et al., 2022).

83 Following the discovery of carbon nanotubes (CNTs) by Sumio Iijima in 1991, it was  
84 observed that CNTs exhibit exceptional performance under mechanical load, thermal environment,  
85 and electric-magnetic loading (Fard, 2021; Fard and Pensky, 2023; Khaniki and Ghayesh, 2020; Roy  
86 et al., 2015, 2014). Numerous studies predicted CNT reinforced composites with functional graded  
87 distribution profiles perform well under bending but random distribution is considered to be a more  
88 practical distribution profile in terms of manufacturing of laminates. The present study examines the  
89 stability performance of shell panels reinforced with CNTs that are randomly distributed while  
90 considering the agglomeration impact of nanotubes in the polymer matrix. To improve the strength,  
91 fibers are added in the hybrid matrix (CNT and Polymer) that results in a multiphase composite. The  
92 behavior of CNT-reinforced flat panels under transverse and in-plane loads have been studied by  
93 several researchers and it can be observed that functional gradation with an X distribution pattern  
94 provides the maximum stiffness against bending (opposite for the O distribution pattern). This is  
95 because the density of nanotubes is highest at the surface and lowest near the neutral axis for the X  
96 distribution (Ansari et al., 2018; Chakraborty et al., 2021; Kiani and Mirzaei, 2018; Shen and Zhang,  
97 2010; Shen, 2012). Ansari et al. (2016) investigated the stability of functionally graded conical shell  
98 panels by using the Variational Differential Quadrature (VDQ) technique. First-order shear

deformation theory (FSDT) was used to develop the strain-displacement model of the shell panel, and the Hamilton variational approach was used to construct the governing equations. The stability of Piezoelectric CNT-reinforced cylindrical panels was analyzed by Nasihatgozar et al. (2016). The effective material properties of functionally graded CNT composites were determined using the Eshelby-Mori-Tanaka approach and the Donnell shell theory was used to model the panel. The kp-Ritz meshless technique along with the arc-length method was used to trace the non-linear equilibrium path of CNT-reinforced cylindrical shell panels by Liew et al. (2014). It has been observed that the panel follows a non-linear equilibrium path with a softening phase initially and then hardening in the later stage. A finite element approach was presented by Gracia et al. (2017a, 2017b) to obtain the stability characteristics of the FG-CNTRC cylindrical shell panels subjected to axial loadings and the effective material properties of composites were obtained using the Eshelby-Mori-Tanaka technique. Zghal et al. (2018) presented a finite element shell model considering the higher-order shear theory to investigate the FG-CNTRC curved panel stability characteristics. The authors observed significant improvement in buckling load due to the gradation of nanotubes and presented the stability response for various parametric properties. Chakraborty et al. (2019), using a semi-analytical solution, investigated the non-linear stability of a functional graded cylindrical shell panel subjected to non-uniform and localized loadings. It has been observed that the panel will deform continuously due to the tensile stresses developed in the transverse direction of the applied load. FG-CNTRC cylindrical shell panels' buckling stresses under an in-plane load were estimated using the stable space approach by Liew and Alibeigloo (2021). The authors observed, that the panel with FG-X pattern exhibits minimum in-plane stresses and vice-versa for FG-O profile. The stability behavior of a cylindrical panel with an internal cutout was studied by Reddy and Ram (2021) using the finite element method. The finding reveals that the FG- X and FG-O pattern performs well as compared to other distributions and with an increase in cutout size the buckling load decreases.

The investigations concerning the stability of CNT-reinforced composites is limited, particularly focusing on the effects of some of the practical and inevitable phenomenon like agglomeration. Shi et al. (2004) discussed the procedure to estimate the resulting material properties

126 of randomly dispersed CNT-reinforced composites through the Eshelby-Mori-Tanaka  
127 micromechanical technique. Forougi et al. (2013) presented the stability performance of a randomly  
128 dispersed nanotube-reinforced polymer-fiber composite resting on an elastic foundation. The  
129 effective material properties were obtained using Mori-Tanaka micromechanical modeling and it was  
130 observed that with an increase in the volume fraction of nanotubes the non-dimensional buckling  
131 load increases. Arani et al. (2011) presented a finite element model to investigate the stability  
132 performance of randomly distributed CNT in a matrix considering the agglomeration effect. It was  
133 observed that an increase in agglomeration leads to a decrease in buckling strength when the panel is  
134 subjected to axial load. The influence of CNTs waviness and agglomeration with the inclusion of  
135 polymer matrix was considered in the design parameters of CNT-polymer composites by  
136 Georgantzinos et al. (2021) using FEM. Recent research has focused on the stability of RD-CNTRC  
137 plate and shell panels by considering sinusoidal shear deformation theory to model these panels  
138 (Daghigh et al., 2020; Georgantzinos et al., 2021). Dastjerdi and Malek-Mohammadi (2017)  
139 proposed a higher-order displacement theory along with Navier's approach to model sandwich plates  
140 reinforced with RD-CNTRC face sheets subjected to bi-axial loadings. Sandwich CNTRC plate  
141 stability under a hygro-thermal environment was studied by Kiarasi et al. (2020) using Classical  
142 Laminated Plate Theory (CLPT). The influence of agglomeration was considered by obtaining the  
143 effective material properties using the Mori-Tanaka Approach. Safaei et al. (2019) modeled material  
144 properties of CNTRC sandwich plates by considering temperature sensitivity and obtained buckling  
145 response using a meshfree technique. The authors designed porosity in the core by considering  
146 gradation along the thickness of the plate. In a subsequent article (Moradi-Dastjerdi et al., 2020)  
147 stability of porous CNTRC sandwich plates was studied with two piezo-electric facesheets and  
148 subjected to thermo-mechanical loading.

149 Fantuzzi et al. (2020) and Tornabene (2019) presented homogenization techniques to define  
150 the resulting material properties of three-phase randomly dispersed CNT-reinforced composite plate  
151 and shell panels. Following these homogenization techniques, Baccocchi (2020) obtained the critical  
152 load of the multi-phase CNT-reinforced fiber composites. Based on experimentally obtained elastic

153 properties of multi-walled CNT-reinforced fiber composites, Kamarian et al. (2020) investigated  
154 stability characteristics using the general differential quadrature (GDQ) approach. Thermal non-  
155 linear stability analysis was carried out for multi-phase shape memory alloy (SMA) fiber composites  
156 reinforced with CNTs by Mehar et al. (2021a) using the finite element approach. Some recent studies  
157 investigated the stability characteristics of randomly dispersed CNT-reinforced fiber composite  
158 structures like beam, plate, and shell panels using semi-analytical approaches (Chakraborty et al.,  
159 2022b, 2022a; Dash et al., 2022).

160 The stability of flat and cylinder-shaped CNTRC panels was primarily covered in the above-  
161 mentioned studies, whereas the current study's focus is to investigate the nonlinear stability of  
162 various shell panels, followed by the possibility of exploiting geometry-dependent programmable  
163 features. In this section, a detailed review of the literature on doubly curved panels is framed to  
164 understand the behavioral pattern of doubly curved panels and broadly define the gap of research.  
165 Arefi and Amabili (2021) investigated the buckling characteristics of doubly curved nano-shell  
166 panels by incorporating the sinusoidal transverse shear effect under electro-magneto-elastic loadings.  
167 Post-buckling strength of nanocomposite doubly curved FG-CNTRC shell panels lying on an elastic  
168 foundation in a thermal environment was examined by Duc et al. (2019). The Galerkin approach was  
169 used along with von-Kármán type nonlinearity. The influence of functionally graded doubly curved  
170 shallow shell panels were studied by Dung and Dong (2016) for post-buckling analysis. The shell  
171 panels were modeled using third-order shear deformation theory, which takes geometrical non-  
172 linearities into account. Imperfection in the panel was added for a more realistic portrayal of the shell  
173 panel's non-linear equilibrium path. Huang et al. (2021) modeled micro doubly curved FG-CNTRC  
174 shell panels by considering the transverse shear effect with a higher-order model. It was observed by  
175 the authors that the spherical panels predict maximum buckling strength compared to other panels  
176 and the hyperbolic panel possesses the lowest strength. Investigation of doubly curved shell panel's  
177 stability under a hygro-thermal environment was studied by Karimiasl et al. (2019) using a multi-  
178 scale perturbation technique. The authors carried out the post-buckling analysis for CNT-based,  
179 Graphene-based and Shape memory alloy-based three-phase composites. Panda and co-authors (Kar

et al., 2016; Kar and Panda, 2016; Mahapatra et al., 2016; Mehar et al., 2021b; Panda and Singh, 2013) have made an effort to analyze the non-linear stability and vibration of curved panels in thermal environment. Kumar et al. (2003) studied the buckling and parametric instability of doubly curved panels including tensile patch loading. They observed that spherical panels have high buckling strength compared to other curved panels. The non-linear buckling of doubly curved shallow shell panels under hygrothermal loadings was studied using the finite element approach by Kundu and Han (2009a). The authors obtained the large deformation in panels with temperature increment and multiple deformation modes was observed due to change in moisture content. In a subsequent article (Kundu and Han, 2009b), the authors also studied the vibration and stability characteristics of doubly curved panels under in-plane loads. To trace the non-linear equilibrium path of the shell panel Kundu and Sinha (2007) opted for the incremental iterative arc-length approach. The authors compared the approach with the published works and found a good correlation for both snap-through and snapback behavior. The authors (Kundu et al., 2007) modelled piezo composite doubly curved panels and studied the non-linear equilibrium path using a finite element approach. The non-linear static instability of anisotropic laminated doubly curved panels was studied by Li et al. (Li et al., 2021; Liu et al., 2021). A closed-form solution was presented to obtain the non-linear equilibrium path of doubly curved shell panels under out-of-plane loading.

The stability of thin-walled structures has attracted many researchers' interest as discussed in the concise review presented here. The problem gets more difficult for composite materials because of their stacking sequences, complex reinforcement and matrix elements, specific properties of the reinforcements (including irregularities such as agglomeration) along different loading circumstances and boundary conditions. Most of the published works on non-linear stability for curved panels are presented using the finite element approach which normally takes a large computation time. For different structural analyses where multiple realizations of the deterministic model are necessary (such as uncertainty quantification and reliability analysis, sensitivity analysis and optimization), it becomes practically impossible to deal with intensive simulation models (Dey et al., 2018a; Dey et al., 2019; Kumar et al., 2019; Trinh et al., 2020). To reduce such computational time a semi-

analytical approach may be an efficient alternative with adequate physical insights (Haldar et al., 2018). Further, the nonlinear stability of doubly curved three-phase composite shells panels with randomly distributed carbon nanotubes has not been investigated considering the effect of agglomeration and non-uniform in-plane loading. Based on these considerations and identified research gaps, we aim to address the following issues in this article: (a) doubly curvature geometry-dependent (considering spherical, hyperbolic, elliptical and cylindrical panels) modulation of the softening and hardening behavior in the nonlinear stability analysis of three-phase randomly distributed CNT reinforced composite panel, (b) influence of different non-uniform in-plane linear and non-linear loads on non-linear stability of RD-CNTRFC doubly curved panels, (c) influence of CNTs agglomeration on non-linear stability of doubly curved panels, (d) coupled influence of transverse shear stresses (for moderately thick panels) and double curvatures on developing strain-displacement relations, and subsequently analysing the stability behavior. In the context of broader applications, the insights provided in this article, particularly regarding the softening and hardening behaviour of shell panels, would hold significant implications for engineering systems across the length scales. For example, in the realm of energy harvesting, understanding how the structural characteristics of shell panels change under various conditions can be instrumental in optimizing the design of energy harvesting devices. By harnessing these insights, it would become possible to generate optimized voltage output that can be utilized to power sensors and actuators efficiently (Yan et al., 2020), making this knowledge highly valuable for practical applications in the field.

For developing the semi-analytical computational framework of nonlinear stability analysis, the strain-displacement relations would be developed here considering the geometrical nonlinearities of von-Kármán type. The governing equations would subsequently be obtained by minimizing the variation of total energy of the system and the equations would be simplified into algebraic relations using Galerkin's approach. The non-linear equilibrium path of the curved panels would be obtained using Riks-Arc length approach to trace the actual path for load and deflection. The numerical results would explore the aims outlined in the preceding paragraph based on the developed semi-analytical framework.



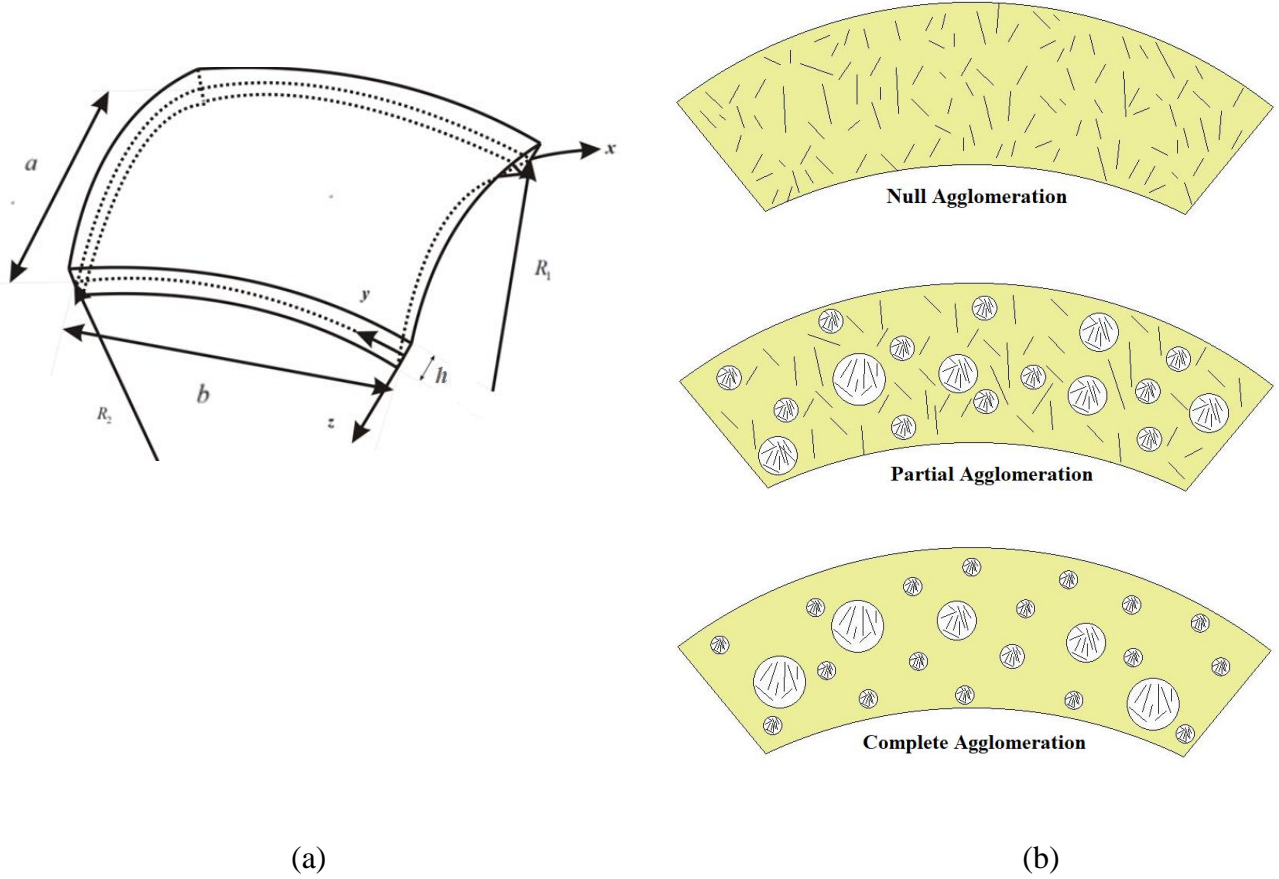


**Fig. 1:** (a) Coordinate system of doubly curved panels; (b) Type of agglomerations.

## 2. Mathematical Formulation

Fig. 1(a) shows the doubly curved panel under consideration having radius of curvature  $R_1$  and  $R_2$  along  $y$  and  $x$  axes, respectively, with plan length of  $a$ , width of  $b$ , and thickness of  $h$ . The panel is constructed with layers of lamina having an identical thickness and bonded together with polymer matrix. The origin of coordinate system is located at the edge of panel mid-layer. Four different geometries of panel are modelled for the present investigation; Spherical Panel ( $R_1 = R, R_2 = R$ ), Cylindrical Panel ( $R_2 = R, R_1 = \infty$ ), Elliptical Panel ( $R_2 = R, R_1 = 2R$ ), and Hyperbolic Panel ( $R_2 = R, R_1 = -R$ ). In the present study, three-phase Fiber/CNT/Polymer composite panel is modelled by assuming the dispersion of CNTs to be random within polymer matrix, resulting in a composition of hybrid matrix where the polymer is further reinforced with straight fibers. Due to improper mixing of nanotubes in matrix polymer, the nanoparticles may form

248 bundles which are known as agglomerations (Shown in Fig. 1(b)). These can be categorized into  
 249 three types: Null agglomeration ( $\alpha = 1; \beta = 1$ ), Partial agglomeration ( $\alpha = 0.5; \beta = 0.75$ ), and  
 250 Complete agglomeration ( $\alpha = 0.5; \beta = 1$ ). Here,  $\alpha$  and  $\beta$  are the agglomeration coefficients.

## 251 2.1 Determination of effective elastic properties of RD-CNTRFC

252 Effective material properties of CNT-reinforced doubly curved composite panels are  
 253 estimated in two stages. Initially, hybrid matrix effective material properties are determined through  
 254 Eshelby-Mori-Tanaka approach, and further Chamis approach is utilized to assess the material  
 255 characteristics of three-phase composites.

256 If  $\bar{V}_{cnt}$  is the CNT fraction in terms of volume present in the entire hybrid matrix volume ( $\bar{V}$ ),  
 257 then the nanotubes can exist both inside and outside of aggregated form of CNT-matrix sphere,  
 258 termed as inclusion. Consequently, the overall CNT volume percent of the hybrid matrix can be  
 259 calculated as (Shi et al., 2004),

$$260 \quad \bar{V}_{cnt} = \bar{V}_{cnt}^{in} + \bar{V}_{cnt}^m \quad (1)$$

261 Here,  $\bar{V}_{cnt}^{in}$  and  $\bar{V}_{cnt}^m$  denote the volume of CNTs inside the inclusion, and the volume of CNTs outside  
 262 the inclusion, respectively. If  $\bar{V}^{in}$  is the total volume of inclusion in the hybrid matrix then the  
 263 agglomeration coefficients ( $\alpha$  and  $\beta$ ) can be expressed as (Shi et al., 2004),

$$264 \quad \alpha = \frac{\bar{V}^{in}}{\bar{V}}; \beta = \frac{\bar{V}_{cnt}^{in}}{\bar{V}_{cnt}} \quad (2)$$

### 265 2.1.1 Eshelby-Mori-Tanaka approach for hybrid matrix

266 Using the Eshelby-Mori-Tanaka (E-M-T) method, the elastic moduli of a hybrid matrix can  
 267 be calculated (Tornabene et al., 2019) as

$$268 \quad K_{hm} = K_{out} \left[ 1 + \frac{\alpha \left( \frac{K_{in}}{K_{out}} - 1 \right)}{1 + \eta_1 (1 - \alpha) \left( \frac{K_{in}}{K_{out}} - 1 \right)} \right] \quad (3)$$

$$G_{hm} = G_{out} \left[ 1 + \frac{\alpha \left( \frac{G_{in}}{G_{out}} - 1 \right)}{1 + \eta_2 (1 - \alpha) \left( \frac{G_{in}}{G_{out}} - 1 \right)} \right] \quad (4)$$

$$\nu_{hm} = \frac{3K_{hm} - 2G_{hm}}{6K_{hm} + 2G_{hm}} \quad (5)$$

$$E_{hm} = \frac{9K_{hm}G_{hm}}{3K_{hm} + G_{hm}} \quad (6)$$

Here,  $\eta_1 = \frac{1 + \nu_{out}}{3(1 - \nu_{out})}$ ,  $\eta_2 = \frac{2(4 - 5\nu_{out})}{15(1 - \nu_{out})}$ . The parameters  $E_{hm}$ ,  $\nu_{hm}$ ,  $G_{hm}$ , and  $K_{hm}$  represent the hybrid matrix elastic properties like Elastic modulus, Poisson's ratio, Shear modulus, and Bulk modulus, respectively. Shear moduli ( $G_{in}$  and  $G_{out}$ ) and Bulk moduli ( $K_{in}$  and  $K_{out}$ ) of inclusion and matrix are presented in Appendix-A.

### 2.1.2 Chamis method for estimation of resulting material properties of randomly distributed CNT reinforced three-phase composites

The obtained hybrid matrix is further fortified with straight fibers, resulting in a three-phase fiber polymer composites. The effective material properties are estimated in the present study using Chamis technique. The volume proportion of fibres and hybrid matrix can be crucial variables to estimate the effective properties. Fibers volume fraction is assumed as  $\bar{V}_f = 0.8$  (Lee, 2018) and the volume proportion of hybrid matrix can be determined using rule of mixture ( $V_{hm} + V_f = 1$ ). Fibers are the reinforcing agent in polymer matrix and they improve the material stiffness. It has been observed in the published study (Lee, 2018) that the in-plane shear modulus can play an important role for the stability of CNT reinforced composite panels. Therefore for accurate non-linear stability analysis of CNT reinforced fiber composites, the volume fraction of fibers should be calibrated for a higher percentage. Considering the influence of in-plane shear modulus in CNT reinforced composites proposed by Lee, 2018, we have considered a higher volume fraction of fibers ( $\bar{V}_f = 0.8$ ) in the present study. The resulting expressions of three-phase composites' elastic constants are

discussed in Appendix-A.

## 2.2 Kinematic relations

Incorporating the transverse shear effect of higher order, proposed by Reddy (HSDT), displacement variables can be expressed as (Reddy, 1984),

$$u(x, y, z, t) = \left(1 + \frac{z}{R_1}\right) u^0(x, y, t) - z w_{,x}^0(x, y, t) + \wp(z) \phi_1(x, y, t) \quad (7)$$

$$v(x, y, z, t) = \left(1 + \frac{z}{R_2}\right) v^0(x, y, t) - z w_{,y}^0(x, y, t) + \wp(z) \phi_2(x, y, t) \quad (8)$$

$$w(x, y, z, t) = w^0(x, y, t) \quad (9)$$

Here, mid-plane displacements are represented as  $u^0$ ,  $v^0$ , and  $w^0$ . The total rotational components can be expressed as,  $\phi_1 = \varphi_x + w_{,x}^0$ ;  $\phi_2 = \varphi_y + w_{,y}^0$ .  $\wp(z) = z \left[ 1 - \left( \frac{4}{3} \right) \left( \frac{z}{h} \right)^2 \right]$  represents the function of

transverse shear.  $\varphi_x$  and  $\varphi_y$  are rotation components of cross-section referring to  $y$  and  $x$ -directions, respectively. Subsequently, the strain-displacement relationship for doubly curved panels can be expressed as (Reddy, 1984),

$$\varepsilon_{xx} = \varepsilon_{xx}^0 - z \left( w_{,xx}^0 - \frac{u_{,x}^0}{R_1} \right) + \wp(z) \phi_{1,x} \quad (10)$$

$$\varepsilon_{yy} = \varepsilon_{yy}^0 - z \left( w_{,yy}^0 - \frac{v_{,y}^0}{R_2} \right) + \wp(z) \phi_{2,y} \quad (11)$$

$$\gamma_{xy} = \gamma_{xy}^0 - z \left( 2w_{,xy}^0 - \frac{u_{,y}^0}{R_1} \right) - z \left( 2w_{,xy}^0 - \frac{v_{,x}^0}{R_2} \right) + \wp(z) \phi_{1,y} + \wp(z) \phi_{2,x} \quad (12)$$

$$\gamma_{xz} = \wp'(z) \phi_1 \quad (13)$$

$$\gamma_{yz} = \wp'(z) \phi_2 \quad (14)$$

Here  $\varepsilon_{xx}^0$ ,  $\varepsilon_{yy}^0$ , and  $\gamma_{xy}^0$  are the mid-plane strains and expressed by considering von-kármán geometrical non-linearities as (Reddy, 1984),

309

$$\boldsymbol{\varepsilon}^0 = \begin{Bmatrix} \varepsilon_{xx}^0 \\ \varepsilon_{yy}^0 \\ \gamma_{xy} \end{Bmatrix} = \begin{Bmatrix} u_{,x}^0 + \frac{w^0}{R_1} + \frac{1}{2} \left( w_{,x}^0 - \frac{u^0}{R_1} \right)^2 \\ v_{,y}^0 + \frac{w^0}{R_2} + \frac{1}{2} \left( w_{,y}^0 - \frac{v^0}{R_2} \right)^2 \\ u_{,y}^0 + v_{,x}^0 + \left( w_{,x}^0 - \frac{u^0}{R_1} \right) \left( w_{,y}^0 - \frac{v^0}{R_2} \right) \end{Bmatrix} \quad (15)$$

310

311

312

The curved panels are composed of multi-layered laminates where local coordinate of each lamina is transformed to global system. The resulting constitutive relations can be presented as (Reddy, 1984),

313

$$\boldsymbol{\sigma}_k = \mathbf{Q}_k \boldsymbol{\varepsilon}_k \quad (16)$$

314

315

316

317

$\boldsymbol{\sigma}_k$  and  $\boldsymbol{\varepsilon}_k$  are the vector representation of  $k^{th}$  layer stress and strain vectors which can be illustrated as  $\boldsymbol{\sigma}_k^T = \{\sigma_{11}, \sigma_{22}, \sigma_{23}, \sigma_{13}, \sigma_{12}\}_k$ ,  $\boldsymbol{\varepsilon}_k^T = \{\varepsilon_{11}, \varepsilon_{22}, \varepsilon_{23}, \varepsilon_{13}, \varepsilon_{12}\}_k$ .  $\mathbf{Q}_k$  is the reduced stiffness matrix for  $k^{th}$  layer of panel and each elements of the matrix can be represented as  $Q_{ij}(i, j=1, 2, 6)$  and along the thickness direction it can be represented as  $Q_{ij}(i, j=4, 5)$  (Reddy, 1984).

318

$$Q_{11} = \frac{E_{11}^c}{1 - \nu_{12}^c \nu_{21}^c}; Q_{12} = \frac{E_{22}^c \nu_{12}^c}{1 - \nu_{12}^c \nu_{21}^c}; Q_{22} = \frac{E_{22}^c}{1 - \nu_{12}^c \nu_{21}^c}; \\ Q_{44} = G_{23}^c; Q_{55} = G_{13}^c; Q_{66} = G_{12}^c \quad (17)$$

319

320

The constitutive equations are then represented in terms of resultant force/moment-strain relations as (Reddy, 1984),

321

$$\mathbf{N} = \mathbf{A} \boldsymbol{\varepsilon}^0 + \mathbf{B} \boldsymbol{\kappa} + \mathbf{C} \boldsymbol{\phi} \quad (18)$$

322

$$\mathbf{M} = \mathbf{B} \boldsymbol{\varepsilon}^0 + \mathbf{C} \boldsymbol{\kappa} + \mathbf{D} \boldsymbol{\phi} \quad (19)$$

323

$$\boldsymbol{\mu} = \mathbf{D} \boldsymbol{\varepsilon}^0 + \mathbf{E} \boldsymbol{\kappa} + \mathbf{F} \boldsymbol{\phi} \quad (20)$$

324

$$\mathbf{V} = \mathbf{H} \boldsymbol{\vartheta} \quad (21)$$

325

326

327

$\mathbf{N}, \mathbf{M}, \boldsymbol{\mu}$ , and  $\mathbf{V}$  are the resultant forces, Moments, Additional moments, and Shear force. Here  $\mathbf{A}$  matrix refers to in-plane stiffness,  $\mathbf{B}$  is the coupling of in-plane and flexure stiffness,  $\mathbf{D}$  matrix represents the flexure stiffness,  $\mathbf{C}$ ,  $\mathbf{E}$ ,  $\mathbf{F}$  are the stiffness contribution due to higher order terms and

328  $\mathbf{H}$  is the stiffness representing the influence of transverse shear stress (defined in Appendix-B).  $\boldsymbol{\kappa}, \boldsymbol{\phi}$ ,  
 329 and  $\boldsymbol{\vartheta}$  are the strains due to bending, additional bending and shear, respectively, as

$$\begin{aligned} \boldsymbol{\kappa}^T &= \left\{ -w_{,xx}^0 + \frac{u_{,x}}{R_1}, -w_{,yy}^0 + \frac{v_{,y}}{R_2}, -2w_{,xy}^0 + \frac{u_{,y}}{R_1} + \frac{v_{,x}}{R_2} \right\}; \boldsymbol{\phi}^T = \{ \phi_{,x}, \phi_{,y}, \phi_{,y} + \phi_{,x} \}; \\ \boldsymbol{\vartheta}^T &= \left\{ \phi_2 - \frac{v}{R_2}, \phi_1 - \frac{u}{R_1} \right\} \end{aligned} \quad (22)$$

331 In terms of stresses, the resultant forces, and moments for  $k^{th}$  layer of laminates can be evaluated as  
 332 (Reddy, 1984),

$$\begin{aligned} \left( \begin{Bmatrix} \mathcal{N}_{xx} \\ \mathcal{N}_{yy} \\ \mathcal{N}_{xy} \end{Bmatrix}, \begin{Bmatrix} M_{xx} \\ M_{yy} \\ M_{xy} \end{Bmatrix}, \begin{Bmatrix} \mu_{xx} \\ \mu_{yy} \\ \mu_{xy} \end{Bmatrix} \right) &= \int_{-h/2}^{h/2} \begin{Bmatrix} \sigma_{xx} \\ \sigma_{yy} \\ \tau_{xy} \end{Bmatrix} (1, z, \wp(z)) dz = \sum_{k=1}^n \int_{z_{k-1}}^{z_k} \begin{Bmatrix} \sigma_{xx} \\ \sigma_{yy} \\ \tau_{xy} \end{Bmatrix} (1, z, \wp(z)) dz \\ \begin{Bmatrix} V_{xz} \\ V_{yz} \end{Bmatrix} &= \int_{-h/2}^{h/2} \begin{Bmatrix} \tau_{xz} \\ \tau_{yz} \end{Bmatrix} \wp'(z) dz = \sum_{k=1}^n \int_{z_{k-1}}^{z_k} \begin{Bmatrix} \tau_{xz} \\ \tau_{yz} \end{Bmatrix} \wp'(z) dz \end{aligned} \quad (23)$$

### 334 2.3 Governing partial differential equations

336 The governing partial differential equations can be derived by minimizing the variation of  
 337 energy of the system (Soldatos, 1991; Xiao-Ping, 1996) referring to displacement variables. The  
 obtained partial differential equations for doubly curved RD-CNT reinforced composite panels are

$$\delta u : \hat{\mathcal{N}}_{xx,x} + \hat{\mathcal{N}}_{xy,y} + \left( \frac{M_{xx,x} + M_{xy,y}}{R_1} \right) = 0 \quad (24)$$

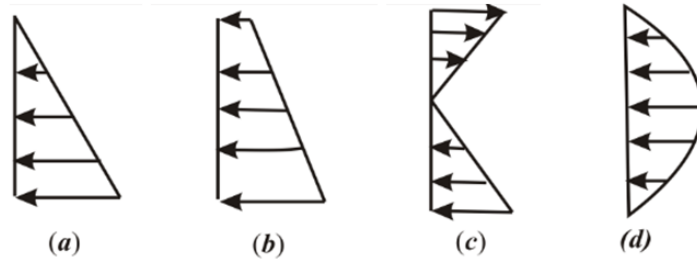
$$\delta v : \hat{\mathcal{N}}_{yy,x} + \hat{\mathcal{N}}_{xy,x} + \frac{(M_{yy,y} + M_{xy,x})}{R_2} = 0 \quad (25)$$

$$\begin{aligned} \delta w : M_{xx,xx} + 2M_{xy,xy} + M_{yy,yy} - \frac{\hat{\mathcal{N}}_{xx}}{R_1} - \frac{\hat{\mathcal{N}}_{yy}}{R_2} + \left[ \hat{\mathcal{N}}_{xx}(w_{,x}) + \hat{\mathcal{N}}_{xy}(w_{,y}) \right]_{,x} \\ + \left[ \hat{\mathcal{N}}_{xy}(w_{,x}) + \hat{\mathcal{N}}_{yy}(w_{,y}) \right]_{,y} = 0 \end{aligned} \quad (26)$$

$$\delta \phi_1 : \mu_{xx,x} + \mu_{xy,y} - V_{xz} = 0 \quad (27)$$

$$\delta \phi_2 : \mu_{xy,x} + \mu_{yy,y} - V_{yz} = 0 \quad (28)$$

344 Here,  $\hat{S}_{xx} = (N_{xx} - n_{xx})$ ,  $\hat{S}_{yy} = (N_{yy} - n_{yy})$ ,  $\hat{S}_{xy} = (N_{xy} - n_{xy})$  and  $n_{xx}$ ,  $n_{yy}$ , and  $n_{xy}$  are the in-plane  
 345 membrane stresses that the panel may experience due to axial non-uniform compression loads. These  
 346 membrane stresses can be determined by satisfying compatibility and edge conditions (the detailed  
 347 determination procedure is discussed in Appendix – C). The present study would investigate non-  
 348 linear stability of doubly curved panels under linear and non-linear in-plane compression loads as  
 349 shown in Fig. 2. The load distribution profile for linearly varying in-plane loads is expressed as:  
 350  $\bar{N}_{xx} = N_0 \left( 1 - \eta \left( \frac{y}{b} \right) \right)$ , and Parabolic in-plane load can be expressed as (Kumar et al., 2016):  
 351  $\bar{N}_{xx} = 4N_0 \left( \frac{y}{b} \right) \left( 1 - \frac{y}{b} \right)$ . Here  $\eta$  is the load factor that represents the linear distribution of in-plane  
 352 loads. It may be noted for linear in-plane loads that the panel may not experience pre-buckling  
 353 stresses as linear in-plane loads match with the neutral axis layer. Thus the investigation of non-  
 354 uniform loading conditions may be critical for stability analysis.



355  
 356 **Fig. 2:** Linear in-plane loads (a) Triangular ( $\eta = 1.0$ ); (b) Trapezoidal ( $\eta = 0.5$ ); (c) Partial Tension  
 357 ( $\eta = 1.5$ ); and (d) Parabolic in-plane load.

#### 358 2.4 Boundary conditions

359 The present methodology can solve for different boundary conditions like all edges are  
 360 clamped (CCCC), alternate clamped (SCSC) and simply-supported edges (CSCS) (Chakraborty et  
 361 al., 2019). For numerical investigation, here the non-linear stability analysis of doubly curved panels  
 362 is performed considering all of the edges as simply supported, and it can be expressed as  
 363 (Chakraborty et al., 2019a),

364 For  $x = 0, a$ :  $n_{xx} - \hat{S}_{xx} = -\bar{N}_{xx}$ ;  $v^0 = w^0 = M_{xx} = \mu_{xx} = \varphi_y = 0$  (29)

365 For  $y = 0, b$ :  $n_{yy} - \hat{S}_{yy} = 0$ ;  $u^0 = w^0 = M_{yy} = \mu_{yy} = \varphi_x = 0$  (30)

The assumed displacement field variables can be obtained by satisfying the above boundary conditions (Chakraborty et al., 2019a),

$$\hat{u} = \sum_{p=1}^P \sum_{q=1}^Q U_{pq} \cos\left(\frac{p\pi x}{a}\right) \sin\left(\frac{q\pi y}{b}\right) \quad (31)$$

$$\hat{v} = \sum_{p=1}^P \sum_{q=1}^Q V_{pq} \sin\left(\frac{p\pi x}{a}\right) \cos\left(\frac{q\pi y}{b}\right) \quad (32)$$

$$\hat{w} = \sum_{p=1}^P \sum_{q=1}^Q W_{pq} \sin\left(\frac{p\pi x}{a}\right) \sin\left(\frac{q\pi y}{b}\right) \quad (33)$$

$$\hat{\phi}_{xx} = \sum_{p=1}^P \sum_{q=1}^Q K_{pq} \cos\left(\frac{p\pi x}{a}\right) \sin\left(\frac{q\pi y}{b}\right) \quad (34)$$

$$\hat{\phi}_{yy} = \sum_{p=1}^P \sum_{q=1}^Q L_{pq} \sin\left(\frac{p\pi x}{a}\right) \cos\left(\frac{q\pi y}{b}\right) \quad (35)$$

Here ( $\hat{\phantom{x}}$ ) represents the approximated displacement variables which depend on finite terms  $p$  and  $q$  along  $x$  and  $y$  directions respectively.

The above displacement field variables [equations (31) – (35)] are substituted in the governing relations [equations (24) - (28)] and further these partial differential equations (PDEs) are simplified into non-linear algebraic equations using Galerkin's approach. Next, the algebraic relations are rearranged in the form of  $\mathbf{K}\boldsymbol{\chi} = 0$ . Here,  $\boldsymbol{\chi}$  is the displacement vector, and  $\mathbf{K}$  is the stiffness matrix. Further  $\mathbf{K}$  can be represented in terms of linear stiffness matrix  $\mathbf{K}_l$  by neglecting non-linear displacement terms, in-plane axial load, and the geometrical stiffness matrix  $\mathbf{K}_g$  containing participation of in-plane load. To obtain these critical buckling loads, the non-linear terms are omitted, and a standard Eigenvalue solution is employed. Furthermore, for the evaluation of non-linear equilibrium paths, the Riks arc-length approach (Vasios, 2015) is utilized, taking into account the non-linear terms in the strain-displacement relationship. It can be noted that neglecting the non-linear terms may not yield very accurate results in non-linear stability analysis for doubly curved panels, while the important behavioral trends can be predicted.



### 3. Result and Discussion

#### 3.1 Comparative analysis and validation

Geometry-dependent non-linear stability of doubly curved panels such as spherical, elliptical, cylindrical, and hyperbolic panels is the focus of this study. In order to trace non-linear equilibrium path of the panel accurately, geometrical non-linearities are introduced when designing the strain-displacement model and transverse shear deformation theory of higher order is taken into account. The accuracy of the current model is established by comparing the critical load of CNTRC panels (Khdeir et al., 1989; Lei et al., 2016; Shadmehri et al., 2012), and non-linear stability of laminated composite shell panels (Girish and Ramachandra, 2006), as available in literature. The effective material properties of hybrid matrix obtained using E-M-T approach are compared with Shi et al. (2004).

In Table 1, the non-dimensional critical load of a flat polymer composite panel reinforced with CNTs subjected to uniaxial and biaxial compressive in-plane loads are compared with the literature. By assuming that nanoparticles are evenly distributed throughout the polymer matrix and the edges are simply supported, the non-dimensional buckling parameter is obtained for various volume fractions of CNTs and compared with the kp-Ritz solution approach based on transverse shear theory of first order (Lei et al., 2016). One can notice that the current method closely matches with the existing literature, wherein the critical load increases as the % CNTs fraction increases. Here,  $N_{xcr}$  represents the instability load for CNT based composite flat panels.

**Table 1.** Non-dimensional critical load  $\left(\frac{N_{xcr}b^2}{E_m h^3}\right)$  of uniformly dispersed CNT flat panel with simply supported edges ( $a/b=1, b/h=10, [0/90/90/0]$ ).

$\bar{V}_{cnt}$	Uniaxial Compression		Biaxial Compression	
	Present	Lei et al. (2016)	Present	Lei et al. (2016)
0.11	20.12	19.84	10.06	9.93
0.14	23.21	22.64	11.60	11.36
0.17	31.29	30.95	15.64	15.49

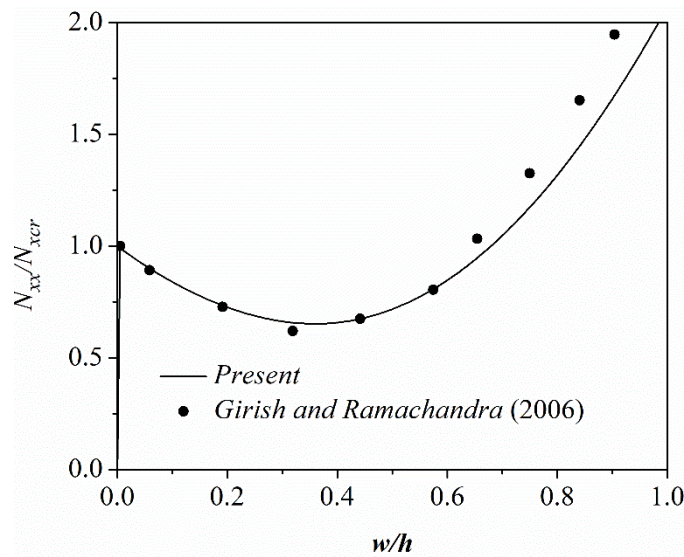
412 **Table 2.** Non-dimensional buckling load  $\left(\frac{N_{xcr}a^2}{100E_{22}h^3}\right)$  of simply supported laminated cylindrical  
 413 shell panel subjected to uniform in-plane compression loads ( $R/h = 10$ ,  $R/a = 1$ ,  $a = b = 1$ ).

Ply Layup	Present	Shadmehri et al. (2012)	Khdeir et al. (1989)
[0/90/0]	0.2754	0.2765	0.2813
[0/90]	0.1703	0.1525	0.1670

414

415 Table 2 shows the non-dimensional buckling load parameter for a laminated cylindrical shell  
 416 panel under in-plane compressive force with simply supported edges. With the help of the current  
 417 method, non-dimensional parameters are obtained for various ply layups and compared with the  
 418 solution obtained using Ritz method considering transverse shear of first order as presented by  
 419 Shadmehri et al. (2012) and higher order transverse shear effect as presented by Khdeir et al. (1989),  
 420 respectively. The current results are in good agreement with the results of published works.

421 Further, the non-linear stability of a laminated cylindrical composite shell is traced and  
 422 compared with the published literature of Girish and Ramachandra (2006), as shown in Fig. 3. It can  
 423 be noticed that the present non-linear stability results show close agreement with the available  
 424 literature. The cylindrical shell panel's non-linear equilibrium response exhibits softening behavior in  
 425 the early stages of deformation and hardening characteristics as the deformation progresses. Such a  
 426 trend is accurately captured by the current computational framework.



427

428 **Fig. 3:** Post-buckling path of simply supported cylindrical shell panel [0/90/90/0] subjected to in-  
 429 plane compression load ( $a/b = 1$ ,  $a/R = 0.38$ ).

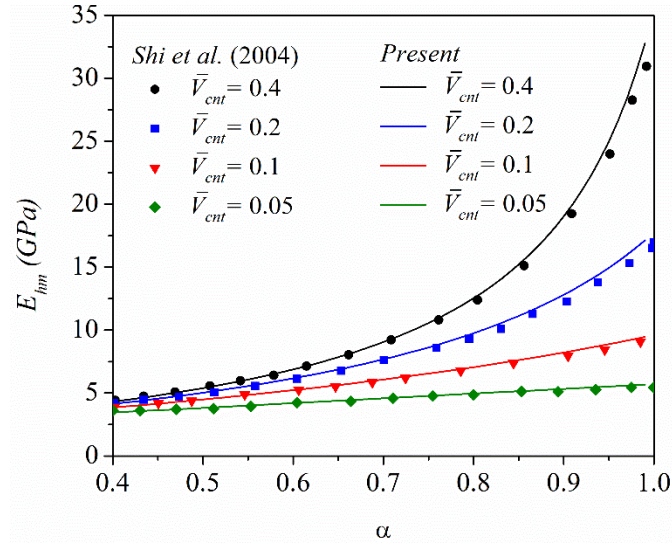


**Fig. 4:** Comparison of effective elastic property of hybrid matrix with an increase in agglomeration of CNTs ( $\beta=1$ ).

After establishing the validations for stability behavior of the shell panels based on the availability of literature (refer to Table 1 – 2 and Fig. 3), we concentrate on the accuracy of the models for obtaining effective material properties of RD-CNT based polymer composites. Fig. 4 shows the comparative results for effective material properties relation given by Shi et al. (2004) for RD-CNT based polymer composites. The material properties are modelled by considering the CNTs agglomeration effect and the elastic modulus of CNT reinforced hybrid polymer composites are seen to decrease with an increase in aggregation of CNTs in polymer, while they increase with % increase of volume content of nanoparticles. To improve the effective elastic properties of CNT reinforced composites, fiber reinforcement has been added to CNT reinforced hybrid matrix which can significantly improve the stiffness property of the composite. In general, a good agreement of the trends can be noticed with respect to published literature.

In this context, it can be noted that a random distribution of nanotubes leads to a heterogeneous mixture, which was also predicted by Shi et al. (2004). In the discussed study by Shi et al. (2004), the authors compared the characteristics of nanotube composites with isotropic and anisotropic properties of nanotubes. They observed that the isotropic characteristics of CNTs may overestimate the tensile modulus of elasticity, which is more pronounced when CNTs are uniformly dispersed in the matrix. Building upon these conclusions, the authors of the present study considered the material properties of nanotubes to be transversely isotropic. Effective material properties are

estimated here using the Mori-Tanaka approach for its simplicity and high accuracy, even at a high volume fraction of inclusions, and also validated with the experimental results by Shi et al., (2004). This approach also takes into account the heterogeneous nature of nanotubes in the matrix. To demonstrate the presence of inhomogeneous behaviour of nanotubes in the polymer matrix, the present micromechanical model considered the agglomeration and dispersion characteristics of nanotubes in the polymer matrix, as shown in Figure 4.

Having validated the computational model from different aspects like the stability behavior and evaluation of effective material properties, we present numerical results concerning the nonlinear stability of doubly curved three-phase composite shells reinforced with randomly distributed carbon nanotubes including the effect of agglomeration in the following subsections. The material properties of CNTs, Polymer and Glass fibers used in the present investigation are mentioned in Table 3.

**Table 3.** Material properties of CNT, matrix, and fiber

<b>SWCNT (10,10)</b>	<b>Glass Fiber properties</b>	<b>Matrix Properties</b>
<b>Hill's Modulus</b> (Singh et al., 2022)	(Chamis, 1983)	<b>(PmPV)</b> (Singh et al., 2022)
$k_{cnt} = 271 \text{ GPa}$	$E_{11}^f = E_{22}^f = E_{33}^f = 73.08 \text{ GPa}$	$E_m = 2.11 \text{ GPa}$
$l_{cnt} = 88 \text{ GPa}$	$G_{12}^f = G_{13}^f = G_{23}^f = 30.13 \text{ GPa}$	$\nu_m = 0.34$
$m_{cnt} = 17 \text{ GPa}$	$\nu_{12}^f = \nu_{13}^f = \nu_{23}^f = 0.22$	
$n_{cnt} = 1089 \text{ GPa}$		
$p_{cnt} = 442 \text{ GPa}$		
<b>Elastic of SWCNT (10,10) (Singh et al., 2022)</b>		
$E_{11}^{cnt} = 5.646 \text{ TPa}; \nu_{12}^{cnt} = 0.175$		

### 3.2 Influence of CNTs agglomeration

The current study examines the non-linear stability of composite shell panels with randomly dispersed CNT reinforcement. The impact of CNT agglomeration on the non-linear stability of several forms of shell panels, such as cylindrical, spherical, elliptical, and hyperbolic, are covered in this section. In Fig. 5, numerical results are presented for panels subjected to uniform in-plane compression loads with simply supported edges. The non-linear equilibrium path of each panel is normalised with the critical load corresponding to null agglomeration of RD-CNTRFC cylindrical

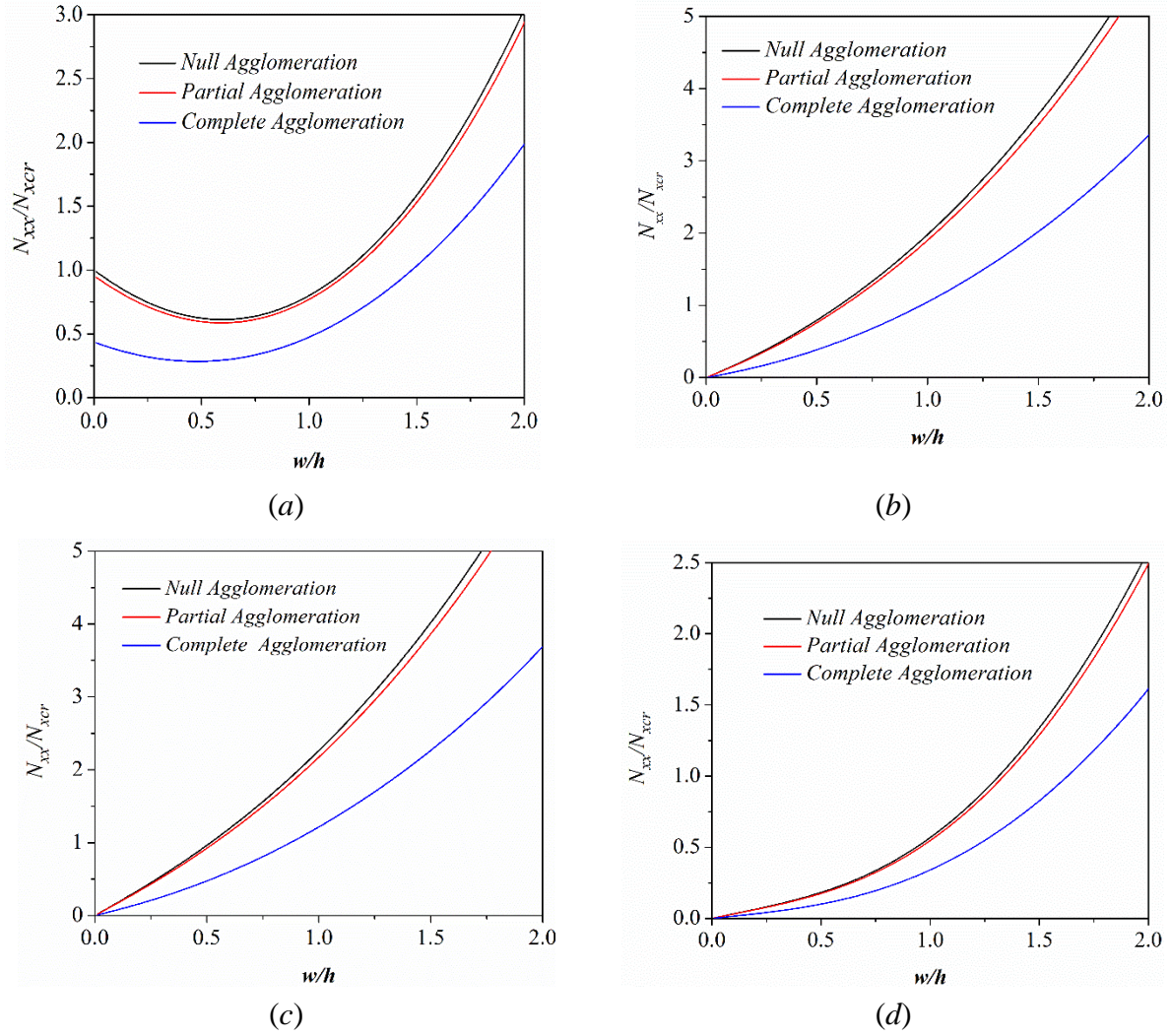


**Fig. 5:** Influence of agglomeration on RD-CNTRFC panels  $[0/90/0/90/0]$  ( $a/b=1, b/h=100, R=10a, w_{cnt}=0.25, \alpha=1, \beta=1$ ) (a) Cylindrical; (b) Spherical; (c) Elliptical; (d) Hyperbolic.

472

473 shell panels. The numerical results reveal that with an increase in CNTs agglomeration, effective  
 474 material properties decrease, resulting in a decrease of the panel stiffness. Therefore, with reference  
 475 to null agglomerations the panel exhibits maximum buckling strength, while the minimum value is  
 476 attained with respect to complete agglomerations. It can be observed that the cylindrical shell panel's  
 477 non-linear equilibrium path starts with bifurcation point and follows a softening behaviour, and  
 478 further deformation leads to hardening behavior. Whereas Spherical, Elliptical and Hyperbolic shell  
 479 panels follow a continuous deformation non-linear equilibrium path due to the tensile stress  
 480 developed in the transverse direction of the panel with the application of in-plane compressive load.  
 481 Such non-unique mechanical characteristics give scope for programming (i.e. application-specific



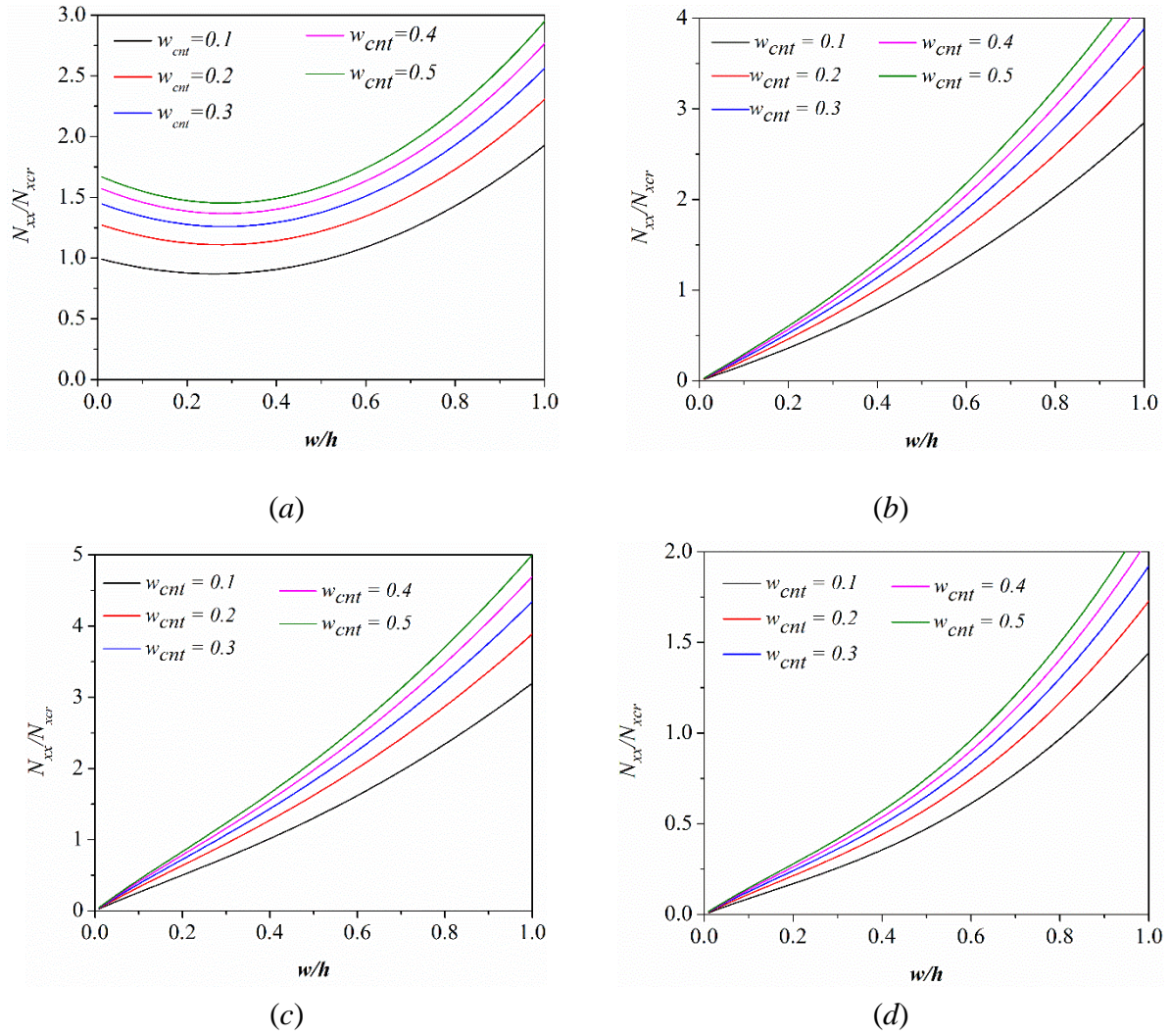


**Fig. 6:** Non-linear stability path of the RD-CNTRFC shell panels  $[0/90/0/90/0]$  for different mass fraction of CNTs ( $a/b=1, b/h=10, R/a=2, \alpha=0.50, \beta=0.75$ ) (a) Cylindrical; (b) Spherical; (c) Elliptical; (d) Hyperbolic.

482

483 designing) the constitutive behaviour of softening and hardening based on the shell geometry for  
 484 application-specific demands.

### 485 3.3 Influence of CNTs mass fraction

486 The influence of CNTs mass fraction on non-linear stability analysis of different shell panels  
 487 is studied in Fig. 6. The panels are simply supported considering the CNTs to be partially  
 488 agglomerated in the hybrid matrix and subjected to uniform in-plane compressive load. The non-  
 489 linear equilibrium path of different panels is normalised with the critical load corresponding to mass  
 490 fraction ( $w_{cnt} = 0.1$ ) of the cylindrical shell panel. It can be observed from Fig. 6 that with an  
 491 increase in mass fraction of CNTs the stiffness of the panels improves, resulting in higher buckling  
 492 strength, but the rate of increase in post-buckling strength with an increase in mass fraction of

493 nanotubes decreases. This happens because the increment of nanotubes in a constant volume of  
 494 polymer matrix tends the nanotubes distribution to agglomerated stage which further reduces the  
 495 effective stiffness of composites and results in a decrease in the rate of enhancing buckling strength  
 496 with an increase of mass fractions of nanotubes. Similar observations are reported in published  
 497 literature (Thirugnanasambantham et al., 2021).

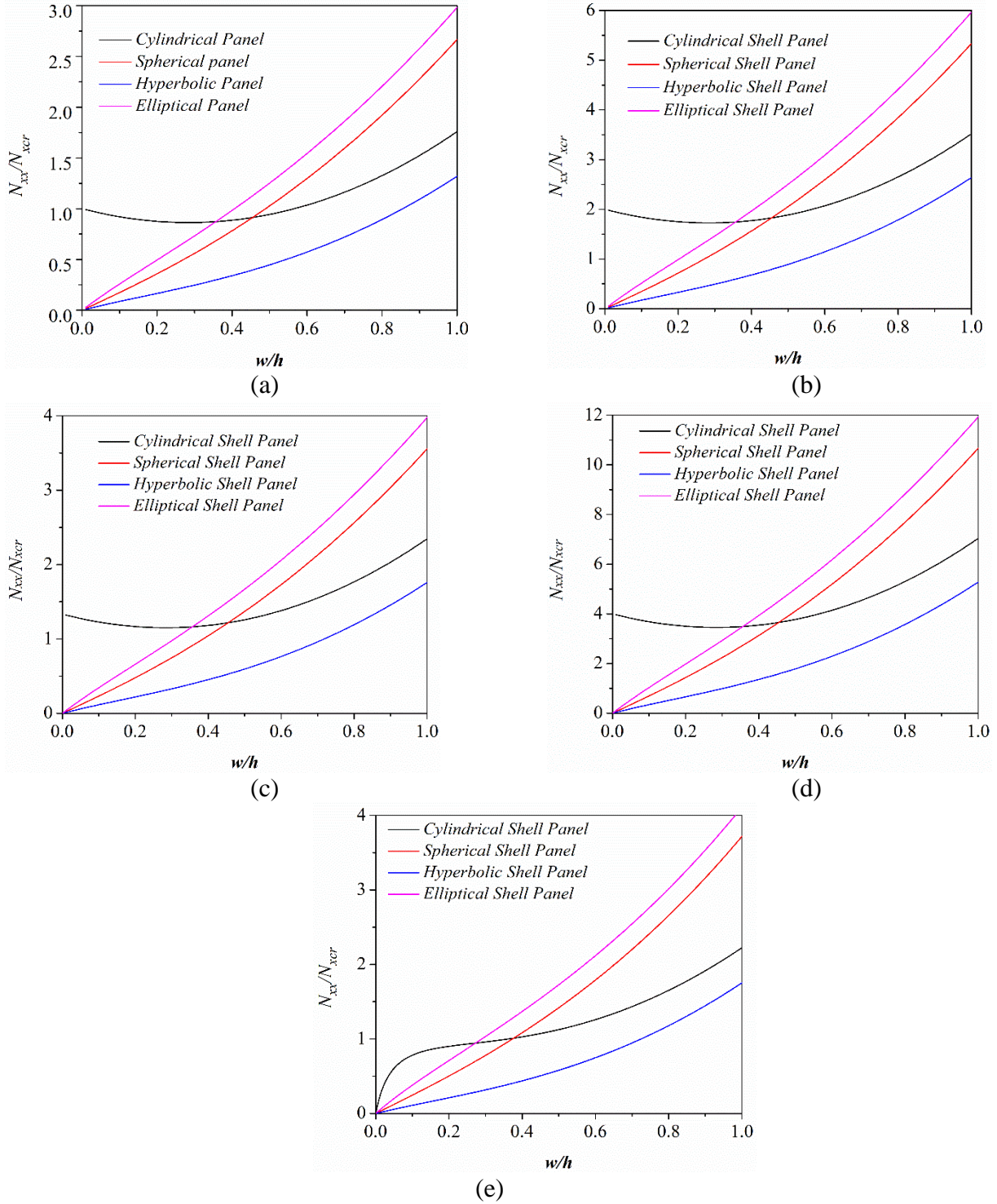


**Fig 7:** Influence of various in-plane compression loads on post-buckling path of different RD-CNTRFC shell panels  $[0/90/0/90/0]$  ( $a/b=1, b/h=10, R/a=2, \alpha=1, \beta=1, w_{cnt}=0.25$ ) (a) Uniform; (b) Triangular; (c) Trapezoidal; (d) Partial Tension; (e) Parabolic.

### 3.4 *Influence of non-uniform in-plane loads*

499 In a practical scenario, it is often unlikely that a shell panel will always be subjected to uniform  
 500 compressive load. To investigate such effects, in this section, the panels are subjected to uniform and  
 501 non-uniform in-plane loads like triangular, trapezoidal, partial tension, and parabolic load variations  
 502 (refer to Fig. 7). For uniform and linear in-plane loads panel does not experience pre-buckling  
 503 stresses as the loads coincide with the panels' neutral axis. But for a parabolic in-plane load, the  
 504 panel will experience the membrane stresses and therefore it has been incorporated for estimation of  
 505 exact stress distribution. The non-linear equilibrium path of each panel is normalised with the critical  
 506 load corresponding to cylindrical shell panel of uniform load distribution. The CNTs in the panel are  
 507 assumed to be properly mixed in the hybrid matrix. It can be noticed that for cylindrical shell panels  
 508 subjected to uniform and linear in-plane loads, the non-linear equilibrium path follows bifurcation  
 509 point. Whereas for cylindrical panels with parabolic in-plane loads, it follows the continuous  
 510 deformation similar to doubly curved panels. This is due to the nature of tensile stress developed in  
 511 the transverse direction to applied in-plane load. It can also be observed that panels subjected to  
 512 partial tensile in-plane load show maximum buckling strength, and the minimum corresponds to  
 513 uniform in-plane loads. It is also noticed that Elliptically curved panels exhibit maximum buckling  
 514 strength, followed by Spherical panel, Cylindrical panel, and minimum corresponds to Hyperbolic  
 515 shell panels (as shown in Fig. 7). In essence, we show in this section that the stability behaviour  
 516 including softening and hardening depends on the coupled effect of shell geometry and nature of in-  
 517 plane loading, which can be programmed based on application-specific demands for most optimal  
 518 performances.

### 519 3.5 *Influence of Radius of curvature of shell panels*

520 Fig. 8 represents the influence of radius of curvature of shell panels on non-linear stability  
 521 path of different shell panels. The non-dimensional ratio for equilibrium paths for the shell panel is  
 522 normalised with critical load corresponding to flat panel when subjected to uniform in-plane  
 523 compressive load. Thus the presented numerical results give a clear perspective on the stability  
 524 behaviour of different shell geometries with respect to the flat plate structure. CNTs are assumed to



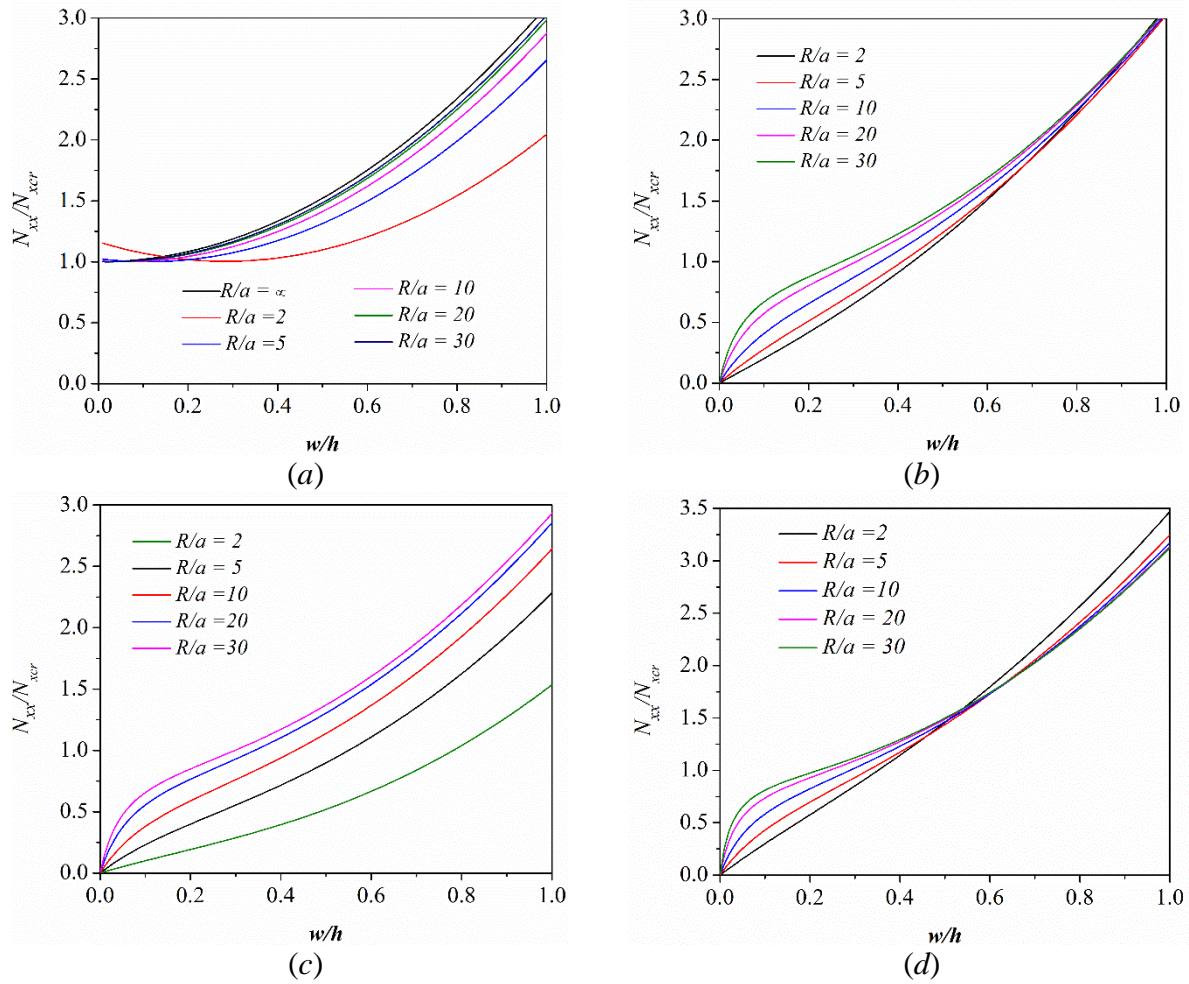


**Fig. 8:** Influence of  $R/a$  ratio on non-linear stability path of different RD-CNTRFC shell panels [0/90/0/90/0] configuration (a) Cylindrical; (b) Spherical; (c) Hyperbolic; (d) Elliptical ( $a/b=1, b/h=10, \alpha=1, \beta=1, w_{crit}=0.25$ ).

525

526 be well mixed with the polymer matrix here. For cylindrical shell panels bifurcation point is  
 527 observed to be on the higher side with the least value of radius-to-span ( $R/a$ ) ratio. With an increase  
 528 of  $R/a$  ratio, the minimum non-dimensional value is observed corresponding to flat panels. For lower  
 529  $R/a$  value, cylindrical panels follow the softening behaviour for the initial non-dimensional  
 530 displacement parameter ( $w/h$ ) and as deformation progresses hardening behaviour can be seen. But  
 531 with an increase in  $R/a$  value softening behaviour in cylindrical panel vanishes. It is also observed in  
 532 cylindrical panels that, with decreasing  $R/a$  value buckling strength also decreases with an increase in  
 533 deformation. Similar behaviour can be noticed for Spherical and Hyperbolic panels, whereas  
 534 Elliptical panels follow the same characteristic for initial  $w/h$  value and in a later stage reverse  
 535 behaviour can be observed. Interestingly, in Spherical panels, the difference in non-linear  
 536 equilibrium path for different  $R/a$  values is found to be insignificant at higher values of  $w/h$ .

Whereas, a significant difference can be observed for Elliptical and Hyperbolic shell panels. At the transition point of softening and hardening behavior of shell panels, stiffness is minimum and corresponding to this stiffness, displacement amplitude can be maximum when a panel is subjected to static and dynamic loads. As an application of the knowledge presented in this article, such softening and hardening behavior can be of significant importance for obtaining the resulting voltage output in energy harvesting devices to operate sensors and actuators (Yan et al., 2020).

In essence, along with the discussions of the preceding subsections, we establish here that a non-linear programming of hardening and softening constitutive behavior is achievable as a function of shell geometry including the radius of curvature and nature of non-uniform loading to address application-specific functional demands optimally. The distribution of CNTs and agglomeration further influence the stability behaviour, albeit not affecting the general trends significantly.

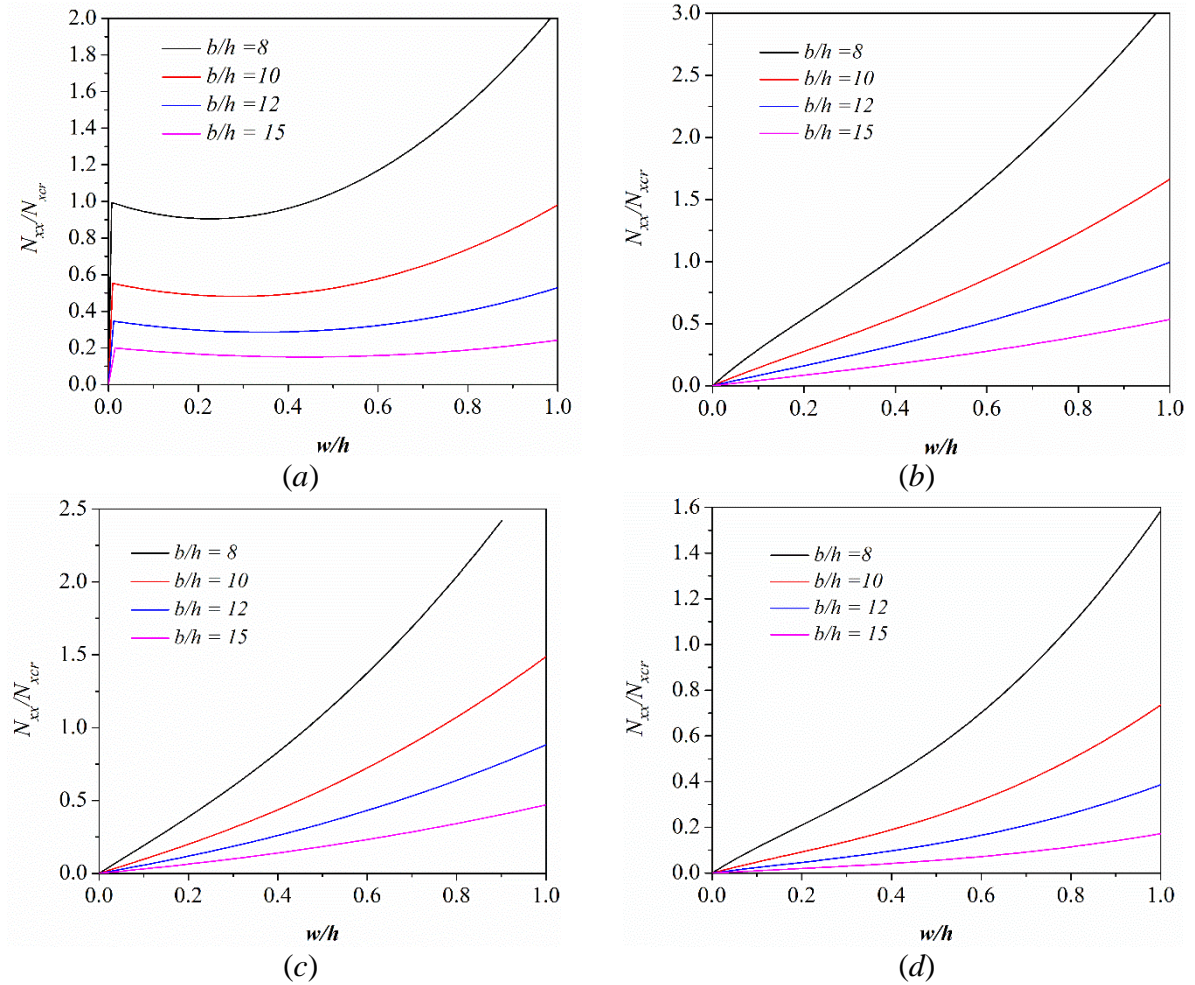


**Fig. 9:** Influence of thickness of shell panels [0/90/0/90/0] subjected to uniform compressive load (a) Cylindrical Panel; (b) Elliptical Panel; (c) Spherical Panel; (d) Hyperbolic Panel ( $a/b=1, R/a=2, \alpha=1, \beta=1, w_{cnt}=0.25$ ).

### 3.6 Influence of thickness of shell panels

Due to the influence of transverse shear effect, thickness of panels is an important parameter to explore the non-linear stability of shell panels. Therefore, the present model is developed to include the higher-order shear theory. The width-to-thickness ratio ( $b/h$ ) of the shell panels is taken into account while modelling them by assuming that the CNT distribution is evenly mixed with the polymer matrix. The non-dimensional parameter is then obtained by normalising the non-linear equilibrium route with the critical load. It can be observed from Fig. 9 that with an increase in width-to-thickness ratio ( $b/h$ ) non-linear equilibrium path of shell panels decreases and this is due to the reduction of panels' stiffness with the decrease of shell panel thickness.

## 4. Conclusions

In the present work, the non-linear equilibrium path is investigated for different doubly curved panel geometries reinforced with randomly distributed CNTs in the polymer matrix. Due to random distribution, the effective material properties and the stability behaviour are significantly influenced which have been investigated including the effect of agglomeration. Along with the parameters involved with CNT distribution and shell geometry, the effect of non-uniform edge loading is explored in this study to understand their coupled influences on the non-linear equilibrium path. Some of the salient conclusions drawn from the numerical analysis are mentioned here

- Panels with complete agglomeration of CNTs show minimum buckling strength compared to null agglomeration. This is due to the reduction of effective material properties of CNT-reinforced fiber composites that result in a reduction of stiffness of composite with an increase of CNTs agglomeration in the polymer matrix.
- Higher stability of the panel is achieved with an increase in mass fraction of CNTs due to an improvement in the stiffness of shell panels. The non-linear equilibrium path of elliptical shell panels exhibits a higher load-deformation path compared to hyperbolic panels.
- It is observed that with an increase of mass fraction of nanotubes, keeping the volume of polymer constant, the non-linear stability of panels improves. However, the rate of increase in non-linear

stability decreases subsequently due to the change of state from null agglomerated to agglomerated phase with an increase in mass fraction of CNTs in polymer matrix resulting in deterioration of materials properties.

- Cylindrical panels follow softening type of non-linear behaviour at the initial non-dimensional deformation ( $w/h$ ) and successive hardening characteristics can be observed at higher value of  $w/h$ . However, the initial softening behaviour is dependent on the radius of curvature and it vanishes with an increase of  $R/a$  value.
- For doubly curved panels non-linear equilibrium path follows continuous deformation with the application of in-plane loads. This is due to the tensile stress developed in the transverse direction with respect to the in-plane applied load.
- Thickness of shell panels significantly influences the non-linear stability characteristics, albeit without altering the general trends significantly. With an increase of shell panel thickness, the panel stiffness also improves resulting in higher stability compared to thin panels.

In summary, multiple shell geometries such as cylindrical, elliptical, spherical and hyperbolic shapes are modelled here along with the flat plate-like geometry, wherein a geometry-dependent programmable softening and hardening behavior emerges with a quantifiable coupled dependence on the non-uniform nonlinear loading condition, shell thickness, radius of curvature and the CNT parameters. Such control on the nonlinear stability behavior of thin-walled structures would lead to enhancing the performance of a multitude of critical engineering applications including energy harvesting, soft robotics, lightweight structural systems and the design of sensors and actuators. Future work in the field of post-buckling for doubly curved panels reinforced with randomly distributed Carbon Nanotubes (CNTs) in the polymer matrix could involve developing new analytical and numerical models, conducting experimental studies to validate theoretical predictions, exploring the potential of using other types of nanoparticles or hybrid reinforcements, investigating the impact of various boundary conditions and loading scenarios, accessing the influence of different defects and progressive damages such as layer-wise debonding (including quantification of the subsequent effect of reduced stiffness), exploring the effect of operating

environment and evaluating the potential applications of these panels in various critical engineering fields.

## Appendix

Appendix-A, Appendix-B and Appendix-C are provided in a supplementary document.

## Acknowledgments

SN and TM would like to acknowledge the initiation grant received from the University of Southampton during the period of this research work.

## Conflict of interest

The authors declare that they have no known competing financial interests or personal relationships that could have appeared to influence the work reported in this paper.

## References

- Ansari, R., Torabi, J., Hassani, R., 2018. In-plane and shear buckling analysis of FG-CNTRC annular sector plates based on the third-order shear deformation theory using a numerical approach. *Comput. Math. with Appl.* 75, 486–502. <https://doi.org/10.1016/j.camwa.2017.09.022>
- Ansari, R., Torabi, J., Shojaei, M.F., Hasrati, E., 2016. Buckling analysis of axially-loaded functionally graded carbon nanotube-reinforced composite conical panels using a novel numerical variational method. *Compos. Struct.* 157, 398–411. <https://doi.org/10.1016/j.compstruct.2016.08.028>
- Arani, A.G., Maghamikia, S., Mohammadimehr, M., Arefmanesh, A., 2011. Buckling analysis of laminated composite rectangular plates reinforced by SWCNTs using analytical and finite element methods. *J. Mech. Sci. Technol.* 25, 809–820. <https://doi.org/10.1007/s12206-011-0127-3>
- Arefi, M., Amabili, M., 2021. A comprehensive electro-magneto-elastic buckling and bending analyses of three-layered doubly curved nanoshell, based on nonlocal three-dimensional theory. *Compos. Struct.* 257. <https://doi.org/10.1016/j.compstruct.2020.113100>
- Baccocchi, M., 2020. Buckling analysis of three-phase CNT/polymer/fiber functionally graded orthotropic plates: Influence of the non-uniform distribution of the oriented fibers on the critical load. *Eng. Struct.* 223, 111176. <https://doi.org/10.1016/j.engstruct.2020.111176>
- Balakrishna Reddy, A., Sai Ram, K.S., 2021. Buckling of functionally graded carbon nanotube reinforced composite cylindrical shell panel with a cutout under uniaxial compression. *Mater. Today Proc.* <https://doi.org/10.1016/j.matpr.2021.08.059>
- Chakraborty, S., Dey, T., Kumar, R., 2021. Instability characteristics of damped CNT reinforced laminated shell panels subjected to in-plane excitations and thermal loading, in: *Structures*. Elsevier, pp. 2936–2949.
- Chakraborty, S., Dey, T., Kumar, R., 2019. Stability and vibration analysis of CNT-Reinforced functionally graded laminated composite cylindrical shell panels using semi-analytical approach. *Compos. Part B Eng.* 168, 1–14. <https://doi.org/10.1016/j.compositesb.2018.12.051>
- Chakraborty, S., Dey, T., Mahesh, V., Harursampath, D., 2022a. Post-buckling and vibration analysis of randomly distributed CNT reinforced fibre composite plates under localised heating. *Mech. Adv. Mater. Struct.* 1–20.
- Chakraborty, S., Dey, T., Singh, V., Kumar, R., 2022b. Thermal Stability Analysis of Three-Phase

643 CNTRFC Cylindrical Shell Panels. *J. Aerosp. Eng.* 35, 4022074.

644 Chamis, C.C., 1983. Simplified Composite Micromechanics equations for Hygral , Thermal and  
645 Mechanical Properties. NASA TM-83320.

646 Chandra, Y., Adhikari, S., Mukherjee, S., Mukhopadhyay, T., 2022. Unfolding the mechanical  
647 properties of buckypaper composites: nano- to macro-scale coupled atomistic-continuum  
648 simulations, *Engineering with Computers*. Springer London. [https://doi.org/10.1007/s00366-](https://doi.org/10.1007/s00366-021-01538-w)  
649 [021-01538-w](https://doi.org/10.1007/s00366-021-01538-w)

650 Daghigh, H., Daghigh, V., Milani, A., Tannant, D., Lacy, T.E., Reddy, J.N., 2020. Nonlocal bending  
651 and buckling of agglomerated CNT-Reinforced composite nanoplates. *Compos. Part B Eng.*  
652 183, 107716. <https://doi.org/10.1016/j.compositesb.2019.107716>

653 Dash, S., Chakraborty, S., Dey, T., Kumar, R., 2022. Buckling and free vibration analysis of  
654 randomly distributed CNT reinforced composite beam under thermomechanical loading. *Eur. J.*  
655 *Mech.* 104749.

656 Dey, S., Mukhopadhyay, T., Adhikari, S., 2018a. Uncertainty quantification in laminated  
657 composites: a meta-model based approach. CRC Press.

658 Dey S., Mukhopadhyay T., Naskar S., Dey T. K., Chalak H. D., Adhikari S., 2019. Probabilistic  
659 characterization for dynamics and stability of laminated soft core sandwich plates, *Journal of*  
660 *Sandwich Structures & Materials*, 21(1) 366 - 397. <https://doi.org/10.1177/1099636217694229>

661 Dey S., Mukhopadhyay T., Sahu S. K., Adhikari S., 2018b. Stochastic dynamic stability analysis of  
662 composite curved panels subjected to non-uniform partial edge loading, *European Journal of*  
663 *Mechanics / A Solids*, 67 108–122. <https://doi.org/10.1016/j.euromechsol.2017.09.005>

664 Duc, N.D., Nguyen, P.D., Cuong, N.H., Van Sy, N., Khoa, N.D., 2019. An analytical approach on  
665 nonlinear mechanical and thermal post-buckling of nanocomposite double-curved shallow shells  
666 reinforced by carbon nanotubes. *Proc. Inst. Mech. Eng. Part C J. Mech. Eng. Sci.* 233, 3888–  
667 3903. <https://doi.org/10.1177/0954406218802921>

668 Fantuzzi, N., Baccocchi, M., Agnelli, J., Benedetti, D., 2020. Three-phase homogenization  
669 procedure for woven fabric composites reinforced by carbon nanotubes in thermal environment.  
670 *Compos. Struct.* 254, 112840. <https://doi.org/10.1016/j.compstruct.2020.112840>

671 Fard, M.Y., 2021. Carbon nanotube network and interphase in buckypaper nanocomposites using  
672 atomic force microscopy. *Int. J. Mech. Sci.* 212, 106811.

673 Fard, M.Y., Pensky, A., 2023. Weibull multiscale interlaminar fracture analysis of low-weight  
674 percentage CNT composites. *Int. J. Mech. Sci.* 250, 108300.

675 Foroughi, H., Askariyeh, H., Azhari, M., 2013. Mechanical Buckling of Thick Composite Plates  
676 Reinforced with Randomly Oriented, Straight, Single-Walled Carbon Nanotubes Resting on an  
677 Elastic Foundation using the Finite Strip Method. *J. Nanomechanics Micromechanics* 3, 49–58.  
678 [https://doi.org/10.1061/\(asce\)nm.2153-5477.0000060](https://doi.org/10.1061/(asce)nm.2153-5477.0000060)

679 García-Macías, E., Rodríguez-Tembleque, L., Castro-Triguero, R., Sáez, A., 2017a. Buckling  
680 analysis of functionally graded carbon nanotube-reinforced curved panels under axial  
681 compression and shear. *Compos. Part B Eng.* 108, 243–256.  
682 <https://doi.org/10.1016/j.compositesb.2016.10.002>

683 García-Macías, E., Rodríguez-Tembleque, L., Castro-Triguero, R., Sáez, A., 2017b. Eshelby-Mori-  
684 Tanaka approach for post-buckling analysis of axially compressed functionally graded  
685 CNT/polymer composite cylindrical panels. *Compos. Part B Eng.* 128, 208–224.  
686 <https://doi.org/10.1016/j.compositesb.2017.07.016>

687 Garg A., Chalak H. D., Sahoo R., Mukhopadhyay T., 2022. Vibration and buckling analyses of  
688 sandwich plates containing functionally graded metal foam core, *Acta Mechanica Solida Sinica*,  
689 35, 1–16. <https://doi.org/10.1007/s10338-021-00295-z>

690 Georgantzinis, S.K., Antoniou, P.A., Giannopoulos, G.I., Fatsis, A., Markolefas, S.I., 2021. Design  
691 of laminated composite plates with carbon nanotube inclusions against buckling: Waviness and  
692 agglomeration effects. *Nanomaterials* 11, 1–23. <https://doi.org/10.3390/nano11092261>

693 Girish, J., Ramachandra, L.S., 2006. Thermomechanical postbuckling analysis of cross-ply laminated  
694 cylindrical shell panels. *J. Eng. Mech.* 132, 133–140. [https://doi.org/10.1061/\(ASCE\)0733-](https://doi.org/10.1061/(ASCE)0733-9399(2006)132)  
695 [9399\(2006\)132](https://doi.org/10.1061/(ASCE)0733-9399(2006)132)

696 Halder, A., Reinoso, J., Jansen, E., Rolfes, R., 2018. Thermally induced multistable configurations of



697 variable stiffness composite plates: Semi-analytical and finite element investigation. *Compos.*  
698 *Struct.* 183, 161–175.

699 Huang, Y., Karami, B., Shahsavari, D., Tounsi, A., 2021. Static stability analysis of carbon nanotube  
700 reinforced polymeric composite doubly curved micro-shell panels. *Arch. Civ. Mech. Eng.* 21,  
701 1–15.

702 Kamarian, S., Bodaghi, M., Isfahani, R.B., Song, J. Il, 2020. Thermal buckling analysis of sandwich  
703 plates with soft core and CNT-Reinforced composite face sheets. *J. Sandw. Struct. Mater.* 0, 1–  
704 39. <https://doi.org/10.1177/1099636220935557>

705 Kar, V.R., Panda, S.K., 2016. Post-buckling behaviour of shear deformable functionally graded  
706 curved shell panel under edge compression. *Int. J. Mech. Sci.* 115–116, 318–324.  
707 <https://doi.org/10.1016/j.ijmecsci.2016.07.014>

708 Kar, V.R., Panda, S.K., Mahapatra, T.R., 2016. Thermal buckling behaviour of shear deformable  
709 functionally graded single/doubly curved shell panel with TD and TID properties. *Adv. Mater.*  
710 *Res.* 5, 205–221. <https://doi.org/10.12989/amr.2016.5.4.205>

711 Karimiasl, M., Ebrahimi, F., Akgöz, B., 2019. Buckling and post-buckling responses of smart doubly  
712 curved composite shallow shells embedded in SMA fiber under hygro-thermal loading.  
713 *Compos. Struct.* 223, 110988. <https://doi.org/10.1016/j.compstruct.2019.110988>

714 Khaniki, H.B., Ghayesh, M.H., 2020. A review on the mechanics of carbon nanotube strengthened  
715 deformable structures. *Eng. Struct.* <https://doi.org/10.1016/j.engstruct.2020.110711>

716 Khdeir, A.A., Reddy, J.N., Frederick, D., 1989. A study of bending, vibration and buckling of cross-  
717 ply circular cylindrical shells with various shell theories. *Int. J. Eng. Sci.* 27, 1337–1351.

718 Kiani, Y., Mirzaei, M., 2018. Rectangular and skew shear buckling of FG-CNT reinforced composite  
719 skew plates using Ritz method. *Aerosp. Sci. Technol.* 77, 388–398.  
720 <https://doi.org/10.1016/j.ast.2018.03.022>

721 Kiarasi, F., Babaei, M., Dimitri, R., Tornabene, F., 2020. Hygrothermal modeling of the buckling  
722 behavior of sandwich plates with nanocomposite face sheets resting on a Pasternak foundation.  
723 *Contin. Mech. Thermodyn.* 1–22. <https://doi.org/10.1007/s00161-020-00929-6>

724 Kumar, R., Dutta, S.C., Panda, S.K., 2016. Linear and non-linear dynamic instability of functionally  
725 graded plate subjected to non-uniform loading. *Compos. Struct.* 154, 219–230.  
726 <https://doi.org/10.1016/j.compstruct.2016.07.050>

727 Kumar R. R., Mukhopadhyay T., Pandey K. M., Dey S., 2019. Stochastic buckling analysis of  
728 sandwich plates: The importance of higher order modes, *International Journal of Mechanical*  
729 *Sciences*, 152 630-643. <https://doi.org/10.1016/j.ijmecsci.2018.12.016>

730 Kundu, C.K., Han, J.H., 2009a. Nonlinear buckling analysis of hygrothermoelastic composite shell  
731 panels using finite element method. *Compos. Part B Eng.* 40, 313–328.  
732 <https://doi.org/10.1016/j.compositesb.2008.12.001>

733 Kundu, C.K., Han, J.H., 2009b. Vibration and post-buckling behavior of laminated composite doubly  
734 curved shell structures. *Adv. Compos. Mater.* 18, 21–42.  
735 <https://doi.org/10.1163/156855108X385320>

736 Kundu, C.K., Maiti, D.K., Sinha, P.K., 2007. Post buckling analysis of smart laminated doubly  
737 curved shells. *Compos. Struct.* 81, 314–322. <https://doi.org/10.1016/j.compstruct.2006.08.023>

738 Kundu, C.K., Sinha, P.K., 2007. Post buckling analysis of laminated composite shells. *Compos.*  
739 *Struct.* 78, 316–324. <https://doi.org/10.1016/j.compstruct.2005.10.005>

740 Lee, S.Y., 2018. Dynamic instability assessment of carbon nanotube/fiber/polymer multiscale  
741 composite skew plates with delamination based on HSDT. *Compos. Struct.* 200, 757–770.  
742 <https://doi.org/10.1016/j.compstruct.2018.05.121>

743 Lei, Z.X., Zhang, L.W., Liew, K.M., 2016. Buckling analysis of CNT reinforced functionally graded  
744 laminated composite plates. *Compos. Struct.* 152, 62–73.  
745 <https://doi.org/10.1016/j.compstruct.2016.05.047>

746 Li, Z.M., Liu, T., Qiao, P., 2021. Buckling and Postbuckling of Anisotropic Laminated Doubly  
747 Curved Panels under Lateral Pressure. *Int. J. Mech. Sci.* 206, 106615.  
748 <https://doi.org/10.1016/j.ijmecsci.2021.106615>

749 Liew, K.M., Alibeigloo, A., 2021. Predicting buckling and vibration behaviors of functionally graded  
750 carbon nanotube reinforced composite cylindrical panels with three-dimensional flexibilities.

Compos. Struct. 256, 113039. <https://doi.org/10.1016/j.compstruct.2020.113039>  
 Liew, K.M., Lei, Z.X., Yu, J.L., Zhang, L.W., 2014. Postbuckling of carbon nanotube-reinforced functionally graded cylindrical panels under axial compression using a meshless approach. *Comput. Methods Appl. Mech. Eng.* 268, 1–17. <https://doi.org/10.1016/j.cma.2013.09.001>  
 Liu, T., Li, Z.M., Qiao, P., 2021. The closed-form solutions for buckling and postbuckling behaviour of anisotropic shear deformable laminated doubly-curved shells by matching method with the boundary layer of shell buckling. *Acta Mech.* 232, 3277–3303. <https://doi.org/10.1007/s00707-021-02952-3>  
 Mahapatra, T.R., Panda, S.K., Kar, V.R., 2016. Geometrically nonlinear flexural analysis of hygro-thermo-elastic laminated composite doubly curved shell panel. *Int. J. Mech. Mater. Des.* 12, 153–171. <https://doi.org/10.1007/s10999-015-9299-9>  
 Mehar, K., Mishra, P.K., Panda, S.K., 2021a. Thermal post-buckling strength prediction and improvement of shape memory alloy bonded carbon nanotube-reinforced shallow shell panel: a nonlinear finite element micromechanical approach. *J. Press. Vessel Technol.* 143, 61301.  
 Mehar, K., Mishra, P.K., Panda, S.K., 2021b. Thermal buckling strength of smart nanotube-reinforced doubly curved hybrid composite panels. *Comput. Math. with Appl.* 90, 13–24. <https://doi.org/10.1016/j.camwa.2021.03.010>  
 Moradi-Dastjerdi, R., Behdinin, K., Safaei, B., Qin, Z., 2020. Buckling behavior of porous CNT-reinforced plates integrated between active piezoelectric layers. *Eng. Struct.* 222. <https://doi.org/10.1016/j.engstruct.2020.111141>  
 Moradi-Dastjerdi, R., Malek-Mohammadi, H., 2017. Biaxial buckling analysis of functionally graded nanocomposite sandwich plates reinforced by aggregated carbon nanotube using improved high-order theory. *J. Sandw. Struct. Mater.* 19, 736–769. <https://doi.org/10.1177/1099636216643425>  
 Nasihatgozar, M., Daghigh, V., Eskandari, M., Nikbin, K., Simoneau, A., 2016. Buckling analysis of piezoelectric cylindrical composite panels reinforced with carbon nanotubes. *Int. J. Mech. Sci.* 107, 69–79. <https://doi.org/10.1016/j.ijmecsci.2016.01.010>  
 Panda, S.K., Singh, B.N., 2013. Large amplitude free vibration analysis of thermally post-buckled composite doubly curved panel embedded with SMA fibers. *Nonlinear Dyn.* 74, 395–418. <https://doi.org/10.1007/s11071-013-0978-5>  
 Ravi Kumar, L., Datta, P.K., Prabhakara, D.L., 2003. Tension buckling and dynamic stability behaviour of laminated composite doubly curved panels subjected to partial edge loading. *Compos. Struct.* 60, 171–181. [https://doi.org/10.1016/S0263-8223\(02\)00314-8](https://doi.org/10.1016/S0263-8223(02)00314-8)  
 Reddy, J.N., 2003. *Mechanics of laminated composite plates and shells: theory and analysis*. CRC press.  
 Reddy, J.N., 1984. Exact solutions of moderately thick laminated shells. *J. Eng. Mech.* 110, 794–809.  
 Roy, S., Das, T., Ming, Y., Chen, X., Yue, C.Y., Hu, X., 2014. Specific functionalization and polymer grafting on multiwalled carbon nanotubes to fabricate advanced nylon 12 composites. *J. Mater. Chem. A* 2, 3961–3970. <https://doi.org/10.1039/c3ta14528j>  
 Roy, S., Das, T., Zhang, L., Li, Y., Ming, Y., Ting, S., Hu, X., Yue, C.Y., 2015. Triggering compatibility and dispersion by selective plasma functionalized carbon nanotubes to fabricate tough and enhanced Nylon 12 composites. *Polymer (Guildf)*. 58, 153–161. <https://doi.org/10.1016/j.polymer.2014.12.032>  
 Safaei, B., Moradi-Dastjerdi, R., Behdinin, K., Qin, Z., Chu, F., 2019. Thermoelastic behavior of sandwich plates with porous polymeric core and CNT clusters/polymer nanocomposite layers. *Compos. Struct.* 226, 111209. <https://doi.org/10.1016/j.compstruct.2019.111209>  
 Shadmehri, F., Hoa, S. V., Hojjati, M., 2012. Buckling of conical composite shells. *Compos. Struct.* 94, 787–792. <https://doi.org/10.1016/j.compstruct.2011.09.016>  
 Shen, H.-S., Zhang, C.-L., 2010. Thermal buckling and postbuckling behavior of functionally graded carbon nanotube-reinforced composite plates. *Mater. Des.* 31, 3403–3411.  
 Shen, H.S., 2012. Postbuckling of functionally graded fiber reinforced composite laminated cylindrical shells, Part I: Theory and solutions. *Compos. Struct.* 94, 1305–1321. <https://doi.org/10.1016/j.compstruct.2011.11.034>



- Shi, D.L., Feng, X.Q., Huang, Y.Y., Hwang, K.C., Gao, H., 2004. The effect of nanotube waviness and agglomeration on the elastic property of carbon nanotube-reinforced composites. *J. Eng. Mater. Technol. Trans. ASME* 126, 250–257. <https://doi.org/10.1115/1.1751182>
- Singh, V., Vescovini, R., Kumar, R., Patel, S.N., Watts, G., 2022. Nonlinear vibration and instability of a randomly distributed CNT-reinforced composite plate subjected to localized in-plane parametric excitation. *Appl. Math. Model.* 101, 453–480.
- Soldatos, K.P., 1991. A refined laminated plate and shell theory with applications. *J. Sound Vib.* 144, 109–129.
- Thirugnanasambantham, K.G., Sankaramoorthy, T., Karthikeyan, R., Kumar, K.S., 2021. A comprehensive review: Influence of the concentration of carbon nanotubes (CNT) on mechanical characteristics of aluminium metal matrix composites: Part 1. *Mater. Today Proc.* 45, 2561–2566. <https://doi.org/10.1016/j.matpr.2020.11.267>
- Tornabene, F., Michele Baccocchi, Fantuzzi, N., Reddy, J.N., 2019. Multiscale Approach for Three-Phase CNT/Polymer/ Fiber Laminated Nanocomposite Structures. *Polym. Compos.* 40, E102–E126. <https://doi.org/10.1002/pc>
- Trinh, M.C., Mukhopadhyay, T., Kim, S.E., 2020. A semi-analytical stochastic buckling quantification of porous functionally graded plates. *Aerosp. Sci. Technol.* 105, 105928. <https://doi.org/10.1016/j.ast.2020.105928>
- Van Dung, D., Thuy Dong, D., 2016. Post-buckling analysis of functionally graded doubly curved shallow shells reinforced by FGM stiffeners with temperature-dependent material and stiffener properties based on TSDT. *Mech. Res. Commun.* 78, 28–41. <https://doi.org/10.1016/j.mechrescom.2016.09.008>
- Vasios, N., 2015. The Arc length method: Formulation, Implementation, and Applications, Harvard education.
- Xiao-Ping, S., 1996. An improved simple higher-order theory for laminated composite shells. *Comput. Struct.* 60, 343–350.
- Yan, Z., Sun, W., Hajj, M.R., Zhang, W., Tan, T., 2020. Ultra-broadband piezoelectric energy harvesting via bistable multi-hardening and multi-softening. *Nonlinear Dyn.* 100, 1057–1077.
- Zghal, S., Frikha, A., Dammak, F., 2018. Mechanical buckling analysis of functionally graded power-based and carbon nanotubes-reinforced composite plates and curved panels. *Compos. Part B Eng.* 150, 165–183. <https://doi.org/10.1016/j.compositesb.2018.05.037>